Volume 16
Number 16
28 April 2024
Pages 7703-8178

Nanoscale

rsc.li/nanoscale

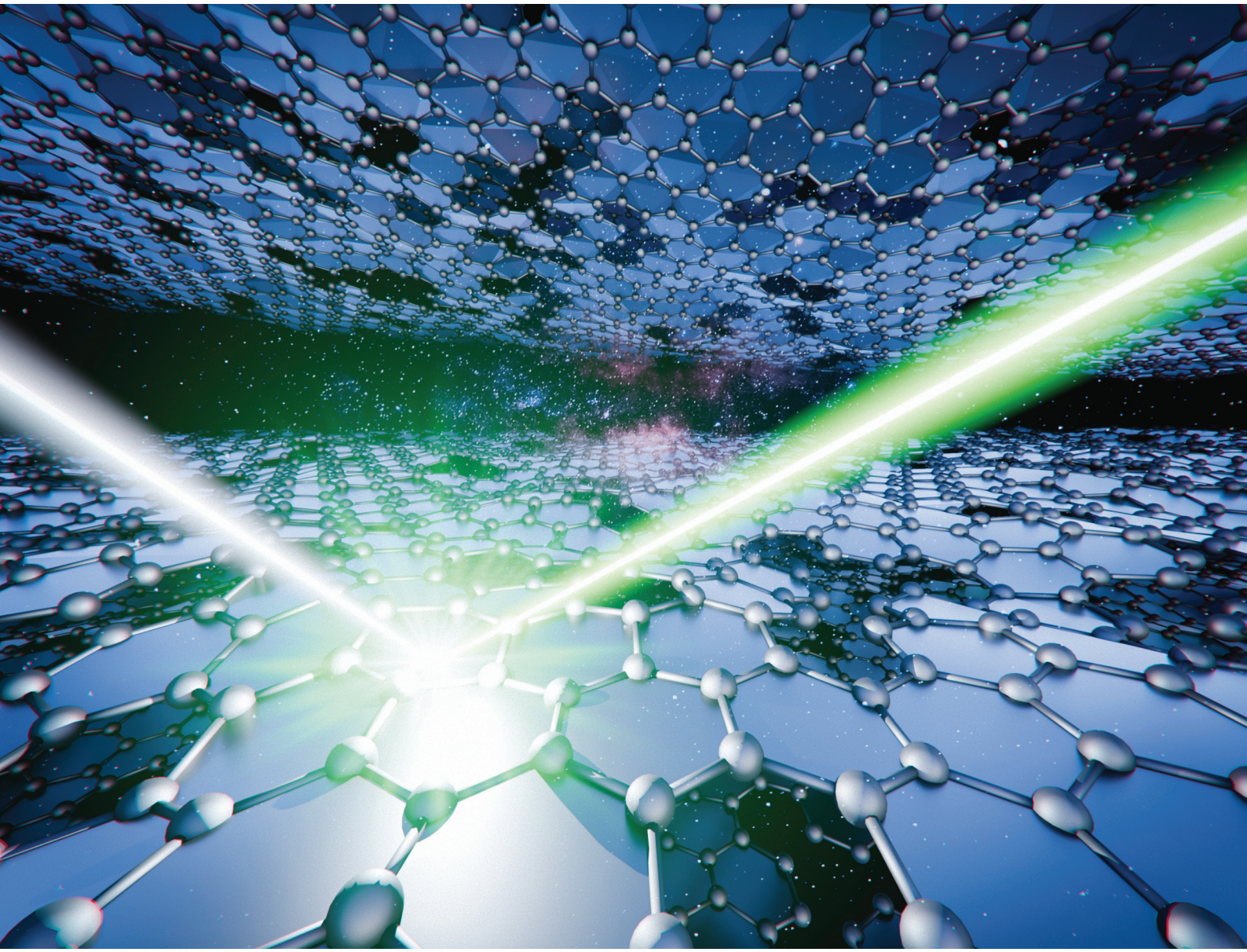

ISSN 2040-3372

ROYAL SOCIETY OF CHEMISTRY

PAPER
Koki Sano *et al.*
A magnetically responsive photonic crystal of graphene oxide nanosheets

NCNST

Nanoscale

ROYAL SOCIETY OF CHEMISTRY

PAPER

View Article Online
View Journal | View Issue

Cite this: *Nanoscale*, 2024, **16**, 7908

A magnetically responsive photonic crystal of graphene oxide nanosheets†

Daisuke Ogawa,[a] Tomoki Nishimura,[a] Yuta Nishina[b] and Koki Sano *[a]

Received 30th November 2023,
Accepted 21st February 2024

DOI: 10.1039/d3nr06114k

rsc.li/nanoscale

Magnetically responsive photonic crystals of colloidal nanosheets hold great promise for various applications. Here, we systematically investigated the magnetically responsive behavior of a photonic crystal consisting of graphene oxide (GO) nanosheets and water. After applying a 12 T magnetic field perpendicular and parallel to the observation direction, the photonic crystal exhibited a more vivid structural color and no structural color, respectively, based on the magnetic orientation of GO nanosheets. The reflection wavelength can be modulated by varying the GO concentration, and the peak intensity can be basically enhanced by increasing both the time and strength of the magnetic application. To improve color quality, we developed a novel approach of alternately applying a magnetic field to two orthogonal directions, instead of using a rotating magnetic field. Finally, we achieved color switching by changing the direction of applied magnetic fields.

Introduction

A photonic crystal, a nanostructure with a periodicity of several hundred nanometers, can selectively reflect light based on Bragg's law, resulting in a structural color.[1–4] This type of color, observed in various organisms and plants, differs from absorption-based colors like dyes and pigments.[5,6] For instance, as used by tropical fish[7,8] and chameleons,[9] the structural color can be modulated by controlling the nanostructure in the photonic crystal.[1–4] Additionally, it is known that certain beetle fossils maintain their structural color without fading even after tens of millions of years.[10,11] Due to the color tunability and fading resistance, functional photonic crystals have found diverse applications in color displays,[12,13] sensors,[14,15] and printing inks.[16,17] Recently, photonic crystals composed of colloidal nanosheets have attracted much attention as a new class of dynamic photonic crystals.[18–41] To manipulate their photonic properties, it is important to control the orientation of nanosheets by applying external stimuli, such as shear forces,[25,26,38] electric fields,[27,28,38–40] and magnetic fields.[29–34] Among these stimuli, a strong magnetic field serves as a promising tool because it can be applied (1) in any direction, (2) with no limitations on size and shape as long as a sample can be placed within a magnetic bore, and (3) in a non-contact manner, avoiding damage to a sample.[29–34] Additionally, it can sometimes orient even diamagnetic nanosheets owing to their anisotropy. Indeed, fascinating functions of photonic crystals comprising titanate nanosheets have been achieved by the control of the nanosheet orientation *via* a strong magnetic field.[31–34] Thus, the investigation of magnetic effects on other nanosheets in photonic crystals will offer possibilities for designing new types of magnetically responsive systems.

Graphene oxide (GO) nanosheets, an oxidized version of graphene, are considered as valuable building blocks for creating functional soft materials due to their large-scale production, low cost, high functionality, and solution processability.[42–47] GO nanosheets are negatively charged

[a]*Department of Chemistry and Materials, Faculty of Textile Science and Technology, Shinshu University, 3-15-1 Tokida, Ueda, Nagano 386-8567, Japan. E-mail: koki_sano@shinshu-u.ac.jp*
[b]*Research Core for Interdisciplinary Sciences, Okayama University, 3-1-1 Tsushimanaka, Kita-ku, Okayama 700-8530, Japan*

†Electronic supplementary information (ESI) available. See DOI: https://doi.org/10.1039/d3nr06114k

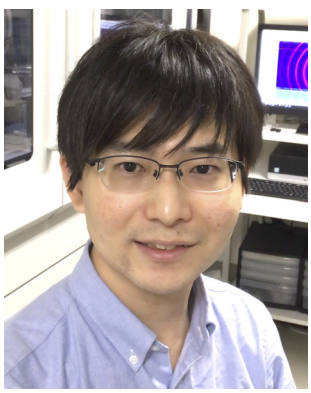

Koki Sano

Koki Sano is an Assistant Professor in the Department of Chemistry and Materials, Faculty of Textile Science and Technology at Shinshu University, Japan. He received his Ph.D. from the University of Tokyo, Japan, in 2019. He worked as a special postdoctoral researcher (SPDR) at RIKEN Center for Emergent Matter Science and a JST PRESTO researcher. His current research interests include the design and construction of functional soft materials and biomimetic systems by using nanomaterials, polymers, and liquid crystals.

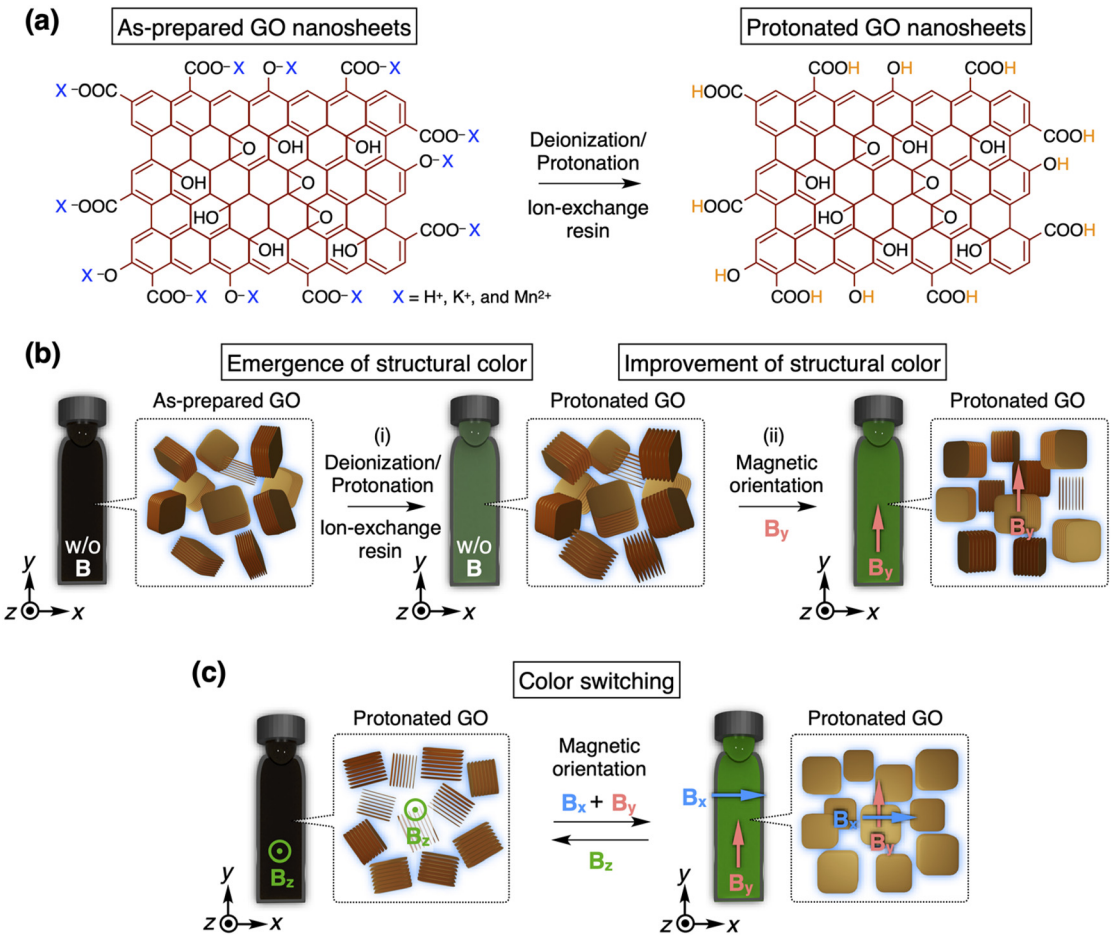

Fig. 1 (a) Schematic illustrations of the preparation method for a photonic crystal of graphene oxide (GO) nanosheets. (b) Schematic illustrations of (i) the emergence of a structural color in an aqueous dispersion of GO nanosheets through deionization/protonation by the addition of an ion-exchange resin and (ii) the improvement of the structural color through the application of a strong magnetic field along the *y*-axis. (c) Schematic illustrations of color switching of the GO dispersion by changing the directions of applied magnetic fields.

owing to their oxygen-containing acidic groups, including acidic hydroxy and carboxy groups, and therefore, they are well dispersed in water (Fig. 1a, left). When the electrostatic repulsion between the GO nanosheets is enhanced by deionization, the periodicity of GO nanosheets expands up to several hundred nanometers, resulting in a photonic crystal that exhibits a structural color.[35–41] Recently, we found that a simple addition of an ion-exchange resin to an aqueous dispersion of GO nanosheets efficiently generates a photonic crystal (Fig. 1a).[41] Although the magnetic control of the orientation of bare graphene and GO nanosheets has successfully led to various functional soft materials,[48–53] the effect of a strong magnetic field on a photonic crystal of bare GO nanosheets has not been systematically studied.

Here, we investigated the magnetically responsive behavior of a photonic crystal consisting of bare GO nanosheets and water. After applying a 12 T magnetic field perpendicular to the observation direction, the photonic crystal exhibited a more vivid structural color due to the magnetic orientation of GO nanosheets (Fig. 1b). The reflection wavelength can be modulated by varying the GO concentration, and the peak intensity can be basically enhanced by increasing both the time and strength of the magnetic application. Furthermore, to improve color quality, we developed a novel approach of alternately applying a magnetic field to two orthogonal directions, instead of using a rotating magnetic field.[52,53] Finally, we succeeded in achieving color switching of the photonic crystal by changing the direction of applied magnetic fields (Fig. 1c). Notably, GO nanosheets align parallel to an applied magnetic field, while titanate nanosheets, a constituent of a reported photonic crystal, align perpendicular to it.[31–34] Therefore, our findings will provide critical insights into the magnetic controllability of photonic crystals of various nanosheets.

Results and discussion

Preparation of a photonic crystal of GO nanosheets

Recently, we developed a facile and reliable method to synthesize GO nanosheets with desired countercations through a two-step reaction.[41] During this work, we discovered that an aqueous dispersion of the as-prepared GO nanosheets tends to

exhibit a vivid structural color after the addition of an ion-exchange resin consisting of a strong acid and base to the GO dispersion. This method is simpler and less time-consuming compared to the conventional approach of using repetitive centrifugation processes.[36–38] According to our method,[41] an aqueous dispersion of the as-prepared GO nanosheets, with a thickness of ~1 nm and a lateral size of ~1 μm, was purified and thoroughly deionized with an ion-exchange resin. During this process, the free ions originating from the oxidation/exfoliation processes of GO nanosheets were removed, and all countercations of the acidic hydroxy and carboxy groups on GO nanosheets were converted to protons (Fig. 1a). As a result, the electrostatic repulsion between the GO nanosheets was enhanced, expanding the periodicity of GO nanosheets enough to selectively reflect visible light (Fig. 1b and i). Thus, the protonated GO nanosheets ([GO] = 0.3 wt%) formed a photonic crystal exhibiting a green structural color (Fig. S1†). Attenuated total reflectance (ATR) FT-IR spectra of the dried thin films of the as-prepared and protonated GO nanosheets and a field emission scanning electron microscopy (FE-SEM) image of the protonated GO nanosheets are shown in Fig. S2 and S3,† respectively.

Magnetic orientation of a photonic crystal of GO nanosheets

In order to investigate the magnetic orientability of the protonated GO nanosheets, we conducted small-angle X-ray scattering (SAXS) measurements at the SPring-8 synchrotron radiation facility. The orientation of GO nanosheets ([GO] = 0.1 wt%) in water was fixed by gelation without the application of a magnetic field *via* photo-polymerization of an acrylic monomer and a crosslinker. Then, the SAXS measurement of the sample was performed to afford an isotropic pattern in the 2D profile, indicating a random orientation of GO nanosheets (Fig. 2a, upper). On the other hand, when the GO orientation was similarly fixed by gelation under a 12 T magnetic field and the SAXS measurements were conducted with the incident X-ray beam directed perpendicular and parallel to the magnetic direction, anisotropic and isotropic patterns were respectively observed in the 2D profiles (Fig. 2b and c, upper). These results suggest that the planes of protonated GO nanosheets in water align parallel to the applied magnetic field. This orientation behavior is consistent with previous studies on the magnetic orientability of GO nanosheets.[51–53] Typically, aromatic molecules, including GO nanosheets, exhibit a significantly larger diamagnetic susceptibility perpendicular to their planes than in the parallel direction due to their aromatic rings, leading to their planes to align parallel to a magnetic field.[54]

Next, we investigated the effect of the magnetic orientation of GO nanosheets on the structural color. Before the magnetic application, an aqueous dispersion of protonated GO nanosheets ([GO] = 0.3 wt%), filled in a 1 mm thick quartz cuvette (40 × 10 × 1 mm), exhibited a green structural color and its reflection spectrum showed a broad peak (Fig. 2a, lower). Subsequently, a 12 T magnetic field was applied to the GO dispersion at room temperature such that the magnetic

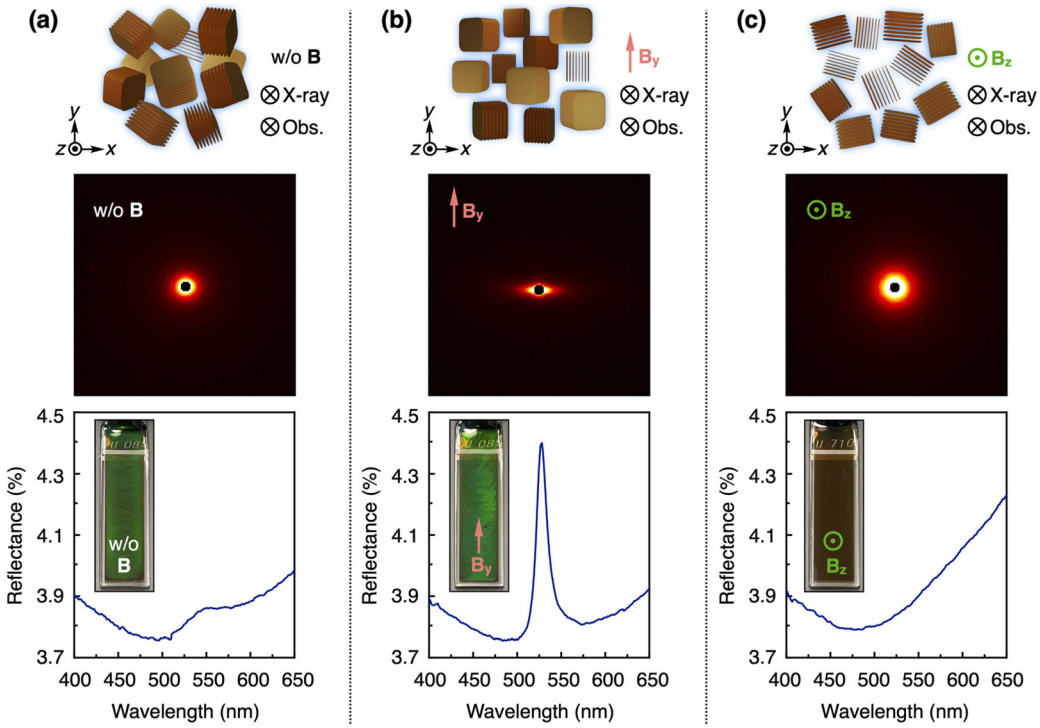

Fig. 2 (a–c) Schematic illustrations of the orientation of GO nanosheets and 2D SAXS profiles of the gel samples of GO nanosheets ([GO] = 0.1 wt%) obtained by photo-polymerization of acrylic monomers and crosslinkers (upper) and reflection spectra (lower) with optical images (inset) of the photonic crystals of GO nanosheets ([GO] = 0.3 wt%) prepared without magnetic application (a) and with a 12 T magnetic application along the *y*-axis (b) and *z*-axis (c).

direction was parallel to the front surface of the cuvette (along the *y*-axis). However, it took more than 9 h to complete the orientation of GO nanosheets (Fig. S4†). To accelerate the orientation time, we conducted the magnetic treatment at 50 °C as follows. A 12 T magnetic field was applied to the GO dispersion at 50 °C for 3 h such that the magnetic direction was parallel (along the *y*-axis) and perpendicular (along the *z*-axis) to the front surface of the cuvette. After cooling to around room temperature for 30 min and removing the magnetic field, we observed the structural color and measured its reflection spectrum. The GO dispersion after the magnetic treatment along the *y*-axis displayed a more vivid green structural color and its reflection spectrum showed a more intense peak (Fig. 2b, lower). These results are attributed to the increased number of planes of GO nanosheets oriented perpendicular to the observation direction (*z*-axis) by the magnetic treatment (Fig. 1b, ii). Such a magnetic orientation behavior of GO nanosheets was confirmed by the above-mentioned SAXS measurements (Fig. 2a and b, upper) and polarized optical observations under crossed nicols (Fig. S5a and S5b†). When the samples were rotated around the *z*-axis, bright birefringence was always observed in the sample before the magnetic application (Fig. S5a†), while the bright/dark contrast of the image changed at every 45° in the sample with the magnetic treatment along the *y*-axis (Fig. S5b†). It should be noted that not all GO nanosheets align perpendicular to the observation direction (*z*-axis) because the planes of GO nanosheets align parallel to the direction of the applied magnetic field (*y*-axis) but can rotate around the magnetic direction (*y*-axis). After the removal of the magnetic field, the reflection peak intensity remained stable for around 25 h and then gradually decreased due to the orientational relaxation of the GO nanosheets (Fig. S6†). When the GO dispersion was magnetically treated along the *z*-axis, almost all planes of GO nanosheets aligned parallel to the observation direction (*z*-axis) and visible light could not be reflected in the *z*-axis direction. As a result, the structural color of the GO dispersion disappeared and its original brown color was observed, with no peak in its reflection spectrum (Fig. 2c, lower). Such a magnetic orientation behavior of GO nanosheets was confirmed by the above-mentioned SAXS measurements (Fig. 2c, upper) and polarized optical observations under crossed nicols, where upon the rotation of the samples around the *z*-axis, bright birefringence was always observed (Fig. S5c†).

Tunability of a photonic crystal of GO nanosheets

First, we studied the effect of the concentration of GO nanosheets ([GO]) on the structural color. By varying the GO concentration from 0.42 to 0.21 wt%, the structural color of the GO dispersion after the magnetic treatment along the *y*-axis changed from blue to green to red (Fig. 3a). The reflection wavelength was modulated from 425 to 660 nm, maintaining a sharp peak in the reflection spectra (Fig. 3b). According to Bragg's law, the red shift of a structural color is derived from the expansion of the nanosheet periodicity with the decrease in the GO concentration due to the strong electrostatic repulsion between GO nanosheets.

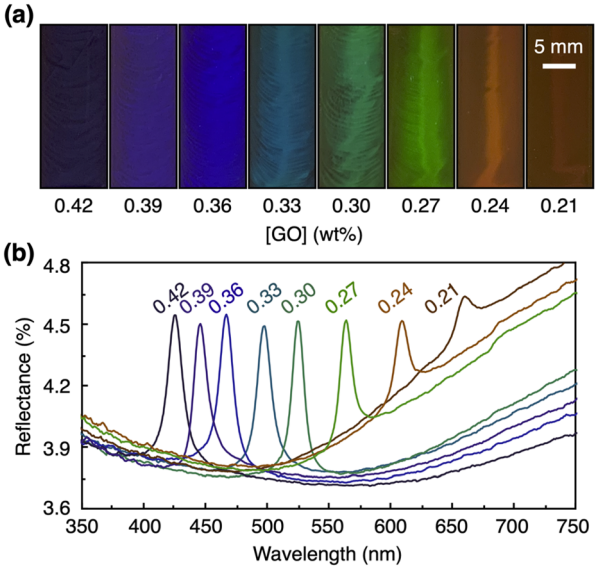

Fig. 3 (a) Optical images and (b) corresponding reflection spectra of the photonic crystals of GO nanosheets with different concentrations ([GO] = 0.21–0.42 wt%) after the magnetic treatment along the *y*-axis.

Next, we systematically investigated the effects of the time (0.5–3.5 h) and strength (0–12 T) of the applied magnetic field on the structural color. The magnetic application time was varied as follows. (1) A 12 T magnetic field was applied to the GO dispersion ([GO] = 0.3 wt%) at 50 °C for 30 min such that the magnetic direction was parallel to the front surface of the cuvette (along the *y*-axis) and was allowed to cool down to around room temperature for 30 min. (2) After the removal of the magnetic field, the reflection spectrum of the sample was measured. (3) This process was repeated to change the total magnetic application time at 50 °C (0.5–3.5 h). The result suggests that the peak intensity of the structural color increased with a longer magnetic application time (Fig. 4a) and reached almost a plateau after 2 h (Fig. 4c). However, we observed that further magnetic application for more than 6 h decreased the peak intensity (Fig. S7a†), possibly because of the heat-induced generation of ionic species, as confirmed by conductivity measurements (Fig. S7b†), and/or gravity-induced orientational changes. By deionization using an ion-exchange resin for 1 h, we successfully removed the ionic species (Fig. S7b†), leading to the recovery of the structural color (Fig. S7a†). When a magnetic field along the *y*-axis with different strengths (0–12 T) was similarly applied to the GO dispersion ([GO] = 0.3 wt%) at 50 °C for 3 h and cooled down to around room temperature for 30 min, the peak intensity of the structural color increased with the larger strength of magnetic application (Fig. 4b and d).

Color switching of a photonic crystal of GO nanosheets

As explained above, the magnetic application in one direction cannot cause all GO nanosheets to align perpendicular to the observation direction because of the free rotation of the planes around the magnetic direction. If all GO nanosheets align per-

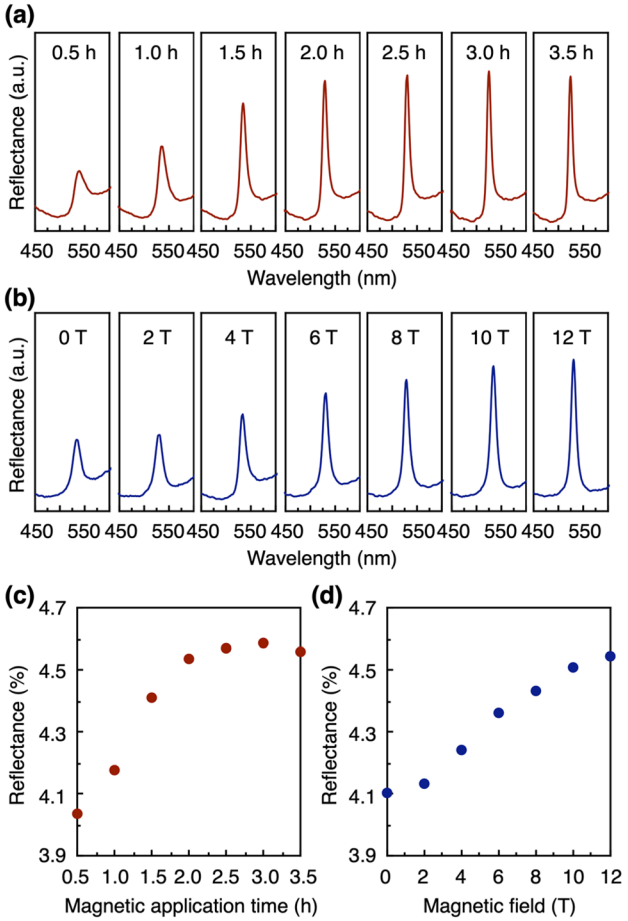

Fig. 4 (a–d) Reflection spectra (a and b) and plots of peak intensity in the spectra (c and d) as a function of the application time of a 12 T magnetic field at 50 °C (a and c) and the magnetic strength with an application time of 3 h (b and d) using a photonic crystal of GO nanosheets ([GO] = 0.3 wt%) with the magnetic treatment along the *y*-axis.

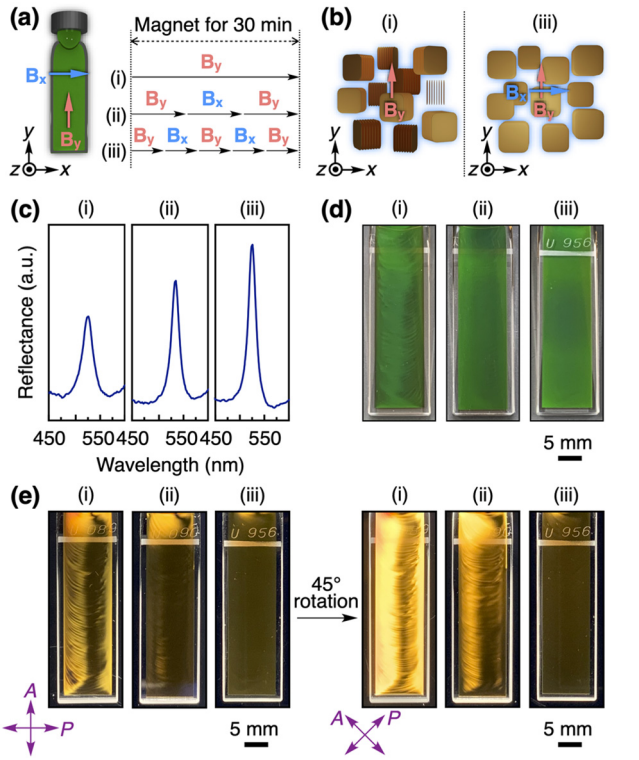

Fig. 5 (a) Magnetic application processes (i–iii) for improving the quality of a structural color. A 12 T magnetic field was alternately applied along the *y*- and *x*-axis directions with a total magnetic application time of 30 min at 50 °C. (b) Schematic illustrations of the orientation of GO nanosheets after processes (i) and (iii). (c) Reflection spectra, (d) optical images, and (e) polarized optical images of a photonic crystal of GO nanosheets ([GO] = 0.3 wt%) after processes (i–iii).

pendicular to the observation direction, they will collectively reflect light, resulting in a more intense and homogeneous structural color. It is known that such an ideal uniaxial orientation of GO nanosheets can be achieved by using a rotating magnetic field, although a special setup is generally required.[52,53] Therefore, we developed an alternative approach of alternately applying a magnetic field to two orthogonal directions.

To confirm the effectiveness of this approach, we applied a 12 T magnetic field to the GO dispersions ([GO] = 0.3 wt%) at 50 °C, where the magnetic directions were as follows: (i) along the *y*-axis for 30 min, (ii) initially along the *y*-axis for 10 min, switched to the *x*-axis for 10 min, and finally returned to the *y*-axis for 10 min, and (iii) initially along the *y*-axis for 6 min, switched to the *x*-axis for 6 min, to the *y*-axis for 6 min, and to the *x*-axis for 6 min, and finally returned to the *y*-axis for 6 min (Fig. 5a). After these processes, the samples were allowed to cool down to around room temperature for 30 min and the subsequent measurements were performed after the removal of the magnetic field. By increasing the number of changes in the magnetic directions, the peak intensity of the structural color increased in its reflection spectrum (Fig. 5c), and the appearance of the structural color became more homogeneous (Fig. 5d). As expected, these changes can be attributed to the increased number of planes of GO nanosheets oriented perpendicular to the observation direction (*z*-axis), as shown in Fig. 5b. Such a magnetic orientation behavior of GO nanosheets was confirmed by polarized optical observations under crossed nicols (Fig. 5e), where upon the rotation of the samples around the *z*-axis, the bright/dark contrast of the image changed at every 45° for the process (i), while the relatively dark and homogeneous image is always observed for the process (iii).

Finally, we aimed to achieve color switching of a photonic crystal of GO nanosheets (Fig. 1c). Initially, a 12 T magnetic field along the *z*-axis was applied to the GO dispersion ([GO] = 0.3 wt%) at 50 °C for 30 min and was cooled down to around room temperature for 30 min (process (iv) in Fig. 6a). Since almost all planes of GO nanosheets aligned parallel to the observation direction (*z*-axis), the structural color was not detected and the original brown color was observed (Fig. 6b). After the magnetic treatment of the sample with the above-mentioned process (iii), as shown in Fig. 5a and 6a, the vivid green structural color appeared (Fig. 6b) because almost all

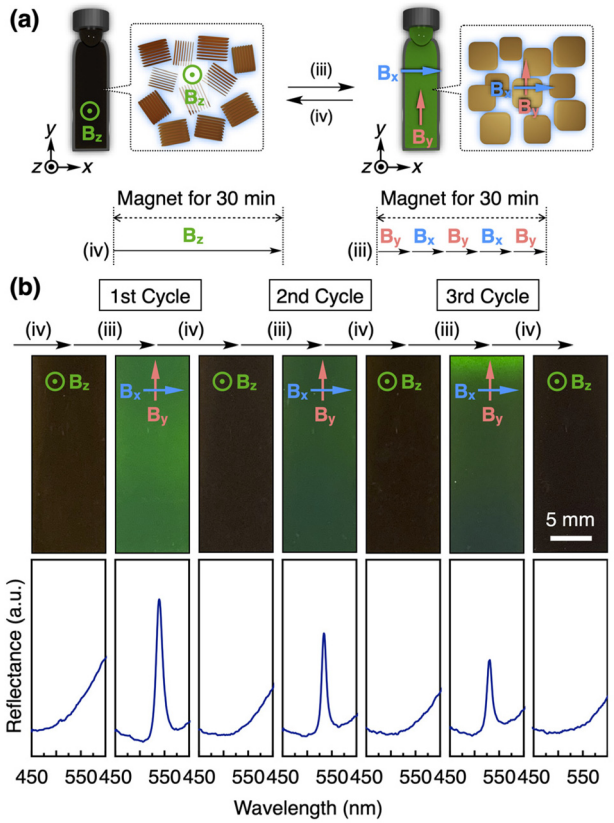

Fig. 6 (a) Magnetic application processes (iii–iv) and their schematic illustrations for color switching. (b) Optical images (upper) and the corresponding reflection spectra (lower) of a photonic crystal of GO nanosheets ([GO] = 0.3 wt%) after repeating processes (iii) and (iv).

planes of GO nanosheets aligned perpendicular to the observation direction (*z*-axis). This color switching can be repeated for three cycles (Fig. 6b), during which we observed a decrease in the peak intensity as the cycle numbers increased. This change might also be attributed to the heat-induced generation of ionic species and/or gravity-induced orientational changes (Fig. S7†). To address this issue, we performed deionization of the photonic crystal of GO nanosheets using an ion-exchange resin and successfully achieved the fully reversible color switching, indicating the potential for further color switching (Fig. S8†).

Conclusions

In summary, we have systematically investigated the magnetically responsive behavior of a photonic crystal consisting of GO nanosheets and water. After applying a 12 T magnetic field along the *y*-axis, it exhibited a more vivid green structural color compared to its pre-treatment state because of the increased number of planes of GO nanosheets oriented perpendicular to the observation direction (*z*-axis). On the other hand, when the photonic crystal was magnetically treated along the *z*-axis, almost all planes of GO nanosheets aligned parallel to the observation direction (*z*-axis), resulting in the disappearance of the structural color and the observation of its original brown color. We also found that the reflection wavelength of the structural color can be modulated from 425 to 660 nm by varying the GO concentration from 0.42 to 0.21 wt%. Furthermore, the peak intensity of structural color can be basically enhanced by increasing both the time and strength of the magnetic application. To achieve a superior quality of the structural color by orienting all GO nanosheets perpendicular to the observation direction (*z*-axis), we developed a novel approach of alternately applying a magnetic field to two orthogonal directions (*x*- and *y*-axes), instead of using a rotating magnetic field.[52,53] This approach successfully realized the ideal uniaxial orientation of GO nanosheets and improved the quality of the structural color. Finally, we accomplished color switching of the photonic crystal by changing the direction of applied magnetic fields.

Compared to typical responsive photonic crystals, the photonic crystal of GO nanosheets offers several advantages as follows. (1) Constituent: GO nanosheets can be synthesized on a large scale and are commercially available. (2) Preparation method: the photonic crystal can be easily prepared by simply adding an ion-exchange resin to an aqueous dispersion of GO nanosheets. (3) Functionality: the functionalization of GO nanosheets could impart additional functions to the photonic crystal. This work demonstrates the utility of a magnetic field as a useful tool for controlling the orientation of nanosheets and the resulting photonic properties. Although the direct use of a 12 T magnetic field might be challenging in practical applications, there is significant potential to reduce the necessary magnetic intensity for manipulating a photonic crystal of GO nanosheets without a superconducting magnet. In such a scenario, our work could provide fundamental insights into magnetic manipulation, leading to various applications, such as color displays,[12,13] sensors,[14,15] and printing inks.[16,17] We believe that these findings will also contribute to expanding the design possibilities of magnetically responsive colloidal systems as well as dynamic photonic crystals composed of various nanosheets.

Experimental section

General and materials

A cryogenic model CFM-12T-100-H3 superconducting magnet with a bore of 100 mm was used for the magnetic orientation of GO nanosheets. A TOMY model CAX-571 centrifuge with a TOMY model CA-16 rotor and a Qsonica model Q125 sonicator were used for the purification of GO nanosheets. Attenuated total reflectance (ATR) FT-IR spectra were recorded on a JASCO model FT/IR-6600 spectrometer. Reflection spectra were recorded with an incident light angle of 5° at room temperature on a JASCO model V-770 spectrophotometer with a JASCO model ARSN-917 manual absolute reflectance measurement unit. Field emission scanning electron microscopy (FE-SEM) was performed by using a JEOL model JSM-IT800SHL.

Conductivity was measured using a Horiba model DS-71E conductivity meter. Water was provided by a Millipore model Milli-Q IQ 7003 water purification system. All reagents were used as received from Tokyo Chemical Industry (TCI) [*N*,*N*-dimethylacrylamide, *N*,*N*′-methylenebisacrylamide, 2-hydroxy-4′-(2-hydroxyethoxy)-2-methylpropiophenone] and Sigma-Aldrich (AmberLite MB mixed ion exchange resin). According to the literature procedure,[45] an aqueous dispersion of GO nanosheets was prepared.

Preparation method of a photonic crystal of GO nanosheets

A photonic crystal of GO nanosheets was prepared as follows.[41] Typically, an aqueous dispersion of the as-prepared GO nanosheets ([GO] = ~0.5 wt%) in a 50 mL centrifuge tube was purified by centrifugation at 6000*g* three times and sonicated for 5 min. Then, we added a 5 wt% ion-exchange resin (AmberLite MB mixed ion exchange resin, Sigma-Aldrich) to the GO dispersion and the dispersion was slowly shaken for more than 24 h. During this process, the free ions originating from the oxidation/exfoliation processes of GO nanosheets were removed and all countercations of the acidic hydroxy and carboxy groups on GO nanosheets were converted to protons (Fig. 1a). As a result, the electrostatic repulsion between the GO nanosheets was enhanced, resulting in a photonic crystal that exhibits a structural color.

Small-angle X-ray scattering (SAXS) measurements

SAXS measurements were carried out at the BL40B2 beamline of SPring-8 synchrotron radiation facility (Hyogo, Japan) using incident X-rays of 1.0 Å wavelength and a 25.4 × 28.9 cm^2 photon-counting detector (PILATUS3 S 2M) with a sample-to-detector distance of 2.1 m. The orientation of GO nanosheets ([GO] = 0.1 wt%) in water was fixed by gelation without the application of a magnetic field (Fig. 2a, upper) and with the application of a 12 T magnetic field for 10 min along the *y*-axis (Fig. 2b, upper) and *z*-axis (Fig. 2c, upper) through *in situ* photo-polymerization for 30 min using an acrylic monomer (*N*,*N*-dimethylacrylamide; 10 wt%), a crosslinker (*N*,*N*′-methylenebisacrylamide; 0.1 wt%), and a photoinitiator (2-hydroxy-4′-(2-hydroxyethoxy)-2-methylpropiophenone; 1 wt%). The resulting 1 mm thick hydrogel samples were subjected to SAXS measurements with the incident X-ray beam directed perpendicular to the front surface of the gel samples.

Magnetic orientation of a photonic crystal of GO nanosheets

After the following magnetic orientations, subsequent observations and measurements were performed after cooling down to around room temperature for 30 min and removing the magnetic field. In Fig. 2b and c, lower, a 12 T magnetic field was applied to a photonic crystal of GO nanosheets ([GO] = 0.3 wt%) in a 1 mm thick quartz cuvette (40 × 10 × 1 mm) at 50 °C for 3 h such that the magnetic direction was parallel (along the *y*-axis) and perpendicular (along the *z*-axis) to the front surface of the cuvette, respectively. In Fig. 3, a 12 T magnetic field was similarly applied to a photonic crystal of GO nanosheets ([GO] = 0.21–0.42 wt%) after the magnetic direction parallel to the front surface of the cuvette (along the *y*-axis). In Fig. 4a and c, the magnetic orientation was performed as follows. (1) A 12 T magnetic field was applied to a photonic crystal of GO nanosheets ([GO] = 0.3 wt%) at 50 °C for 30 min along the *y*-axis and allowed to cool down to around room temperature for 30 min. (2) After the removal of the magnetic field, the reflection spectrum of the sample was measured. (3) This process was repeated to change the total magnetic application time at 50 °C (0.5–3.5 h). In Fig. 4b and d, a magnetic field along the *y*-axis with different strength (0–12 T) was similarly applied to a photonic crystal of GO nanosheets ([GO] = 0.3 wt%) at 50 °C for 3 h. In Fig. 5, a 12 T magnetic field was applied to a photonic crystal of GO nanosheets ([GO] = 0.3 wt%) at 50 °C, where the magnetic directions were as follows: (i) along the *y*-axis for 30 min, (ii) initially along the *y*-axis for 10 min, switched to the *x*-axis for 10 min, and finally returned to the *y*-axis for 10 min, and (iii) initially along the *y*-axis for 6 min, switched to the *x*-axis for 6 min, to the *y*-axis for 6 min, and to the *x*-axis for 6 min, and finally returned to the *y*-axis for 6 min. In Fig. 6, a 12 T magnetic field along the *z*-axis was initially applied to a photonic crystal of GO nanosheets ([GO] = 0.3 wt%) at 50 °C for 30 min and was cooled down to around room temperature for 30 min (process (iv) in Fig. 6a). Next, a 12 T magnetic field was applied to the sample according to the above-mentioned process (iii) in Fig. 5a and 6a. These two magnetic orientations were alternately repeated for three cycles.

Conflicts of interest

There are no conflicts to declare.

Acknowledgements

This work was supported by JST PRESTO Grant Number JPMJPR20A6, Japan (to K. S.) as well as JSPS KAKENHI Grant Numbers JP22H02057 (to K. S.) and JP22H04548 (to Y. N.). K. S. acknowledges the Kurita Water and Environment Foundation (KWEF, Japan). SAXS measurements were performed at the BL40B2 beamline of SPring-8 under proposal number 2023A1121.

References

1 J. Ge and Y. Yin, *Angew. Chem., Int. Ed.*, 2011, **50**, 1492–1522.
2 L. He, M. Wang, J. Ge and Y. Yin, *Acc. Chem. Res.*, 2012, **45**, 1431–1440.
3 P. Liu, L. Bai, J. Yang, H. Gu, Q. Zhong, Z. Xie and Z. Gu, *Nanoscale Adv.*, 2019, **1**, 1672–1685.
4 X. Hou, F. Li, Y. Song and M. Li, *J. Phys. Chem. Lett.*, 2022, **13**, 2885–2900.
5 J. Sun, B. Bhushan and J. Tong, *RSC Adv.*, 2013, **3**, 14862–14889.

6 R. Vaz, M. F. Frasco and M. G. F. Sales, *Nanoscale Adv.*, 2020, **2**, 5106–5129.
7 P. J. Herring, *Comp. Biochem. Physiol., Part A: Mol. Integr. Physiol.*, 1994, **109**, 513–546.
8 D. Gur, B. A. Palmer, B. Leshem, D. Oron, P. Fratzl, S. Weiner and L. Addadi, *Angew. Chem., Int. Ed.*, 2015, **54**, 12426–12430.
9 J. Teyssier, S. V. Saenko, D. van der Marel and M. C. Milinkovitch, *Nat. Commun.*, 2015, **6**, 6368.
10 A. R. Parker, *J. Opt. A: Pure Appl. Opt.*, 2000, **2**, R15–R28.
11 M. E. McNamara, D. E. Briggs, P. J. Orr, H. Noh and H. Cao, *Proc. R. Soc. B*, 2012, **279**, 1114–1121.
12 J. Hou, M. Li and Y. Song, *Angew. Chem., Int. Ed.*, 2018, **57**, 2544–2553.
13 P. Wu, J. Wang and L. Jiang, *Mater. Horiz.*, 2020, **7**, 338–365.
14 C. Fenzl, T. Hirsch and O. S. Wolfbeis, *Angew. Chem., Int. Ed.*, 2014, **53**, 3318–3335.
15 J. Hou, M. Li and Y. Song, *Nano Today*, 2018, **22**, 132–144.
16 B. B. Patel, D. J. Walsh, D. H. Kim, J. Kwok, B. Lee, D. Guironnet and Y. Diao, *Sci. Adv.*, 2020, **6**, eaaz7202.
17 J. Zhang, Y. Qin, Y. Ou, Y. Shen, B. Tang, X. Zhang and Z. Yu, *Angew. Chem., Int. Ed.*, 2022, **61**, e202206339.
18 J.-C. P. Gabriel, F. Camerel, B. J. Lemaire, H. Desvaux, P. Davidson and P. Batail, *Nature*, 2001, **413**, 504–508.
19 M. Wong, R. Ishige, T. Hoshino, S. Hawkins, P. Li, A. Takahara and H.-J. Sue, *Chem. Mater.*, 2014, **26**, 1528–1537.
20 E. Mouri, C. Ogami, T. Fukumoto and T. Nakato, *Chem. Lett.*, 2020, **49**, 717–720.
21 W. Yang, S. Yamamoto, K. Sueyoshi, T. Inadomi, R. Kato and N. Miyamoto, *Angew. Chem., Int. Ed.*, 2021, **60**, 8466–8471.
22 K. El Rifaii, H. H. Wensink, C. Goldmann, L. Michot, J.-C. P. Gabriel and P. Davidson, *Soft Matter*, 2021, **17**, 9280–9292.
23 P. H. Michels-Brito, V. Dudko, D. Wagner, P. Markus, G. Papastavrou, L. Michels, J. Breu and J. O. Fossum, *Sci. Adv.*, 2022, **8**, eabl8147.
24 N. Miyamoto and S. Yamamoto, *ACS Omega*, 2022, **7**, 6070–6074.
25 M. Zeng, D. King, D. Huang, C. Do, L. Wang, M. Chen, S. Lei, P. Lin, Y. Chen and Z. Cheng, *Proc. Natl. Acad. Sci. U. S. A.*, 2019, **116**, 18322–18327.
26 Y. Wang, X. Kan, Y. Liu, J. Ju and X. Yao, *Nanoscale*, 2023, **15**, 9060–9068.
27 A. R. Masud, S.-H. Hong, T.-Z. Shen, A. Shahzad and J.-K. Song, *RSC Adv.*, 2018, **8**, 16549–16556.
28 T.-Z. Shen, K. N. A. Perera, A. R. Masud, P. A. N. S. Priyadharshana, J.-Y. Park, Q.-H. Wang, S.-H. Hong and J.-K. Song, *Cell Rep. Phys. Sci.*, 2023, **4**, 101343.
29 S. Uenuma, R. Maeda, H. Yokoyama and K. Ito, *Chem. Commun.*, 2019, **55**, 4158–4161.
30 C. Zhang, Z. Wu, Z. Chen, L. Pan, J. Li, M. Xiao, L. Wang, H. Li, Z. Huang, A.-B. Xu, C. Li and L. He, *J. Mater. Chem. C*, 2020, **8**, 16067–16072.
31 K. Sano, Y. S. Kim, Y. Ishida, Y. Ebina, T. Sasaki, T. Hikima and T. Aida, *Nat. Commun.*, 2016, **7**, 12559.
32 K. Sano, Y. O. Arazoe, Y. Ishida, Y. Ebina, M. Osada, T. Sasaki, T. Hikima and T. Aida, *Angew. Chem., Int. Ed.*, 2018, **57**, 12508–12513.
33 K. Sano, X. Wang, Z. Sun, S. Aya, F. Araoka, Y. Ebina, T. Sasaki, Y. Ishida and T. Aida, *Nat. Commun.*, 2021, **12**, 6771.
34 Y.-Y. Zhan, D. Ogawa, K. Sano, X. Wang, F. Araoka, N. Sakai, T. Sasaki and Y. Ishida, *Angew. Chem., Int. Ed.*, 2023, e202311451.
35 P. Li, M. Wong, X. Zhang, H. Yao, R. Ishige, A. Takahara, M. Miyamoto, R. Nishimura and H.-J. Sue, *ACS Photonics*, 2014, **1**, 79–86.
36 Y.-T. Xu, U. V. Mody and M. J. MacLachlan, *Nanoscale*, 2021, **13**, 7558–7565.
37 Y.-T. Xu, J. Li and M. J. MacLachlan, *Nanoscale Horiz.*, 2022, **7**, 185–191.
38 T.-Z. Shen, S.-H. Hong, B. Lee and J.-K. Song, *NPG Asia Mater.*, 2016, **8**, e296.
39 S.-H. Hong, T.-Z. Shen and J.-K. Song, *Opt. Express*, 2015, **23**, 18969–18974.
40 T. K. Ekanayaka, S.-H. Hong, T.-Z. Shen and J.-K. Song, *Carbon*, 2017, **123**, 283–289.
41 S. Kondo, T. Nishimura, Y. Nishina and K. Sano, *ACS Appl. Mater. Interfaces*, 2023, **15**, 37837–37844.
42 S. Eigler and A. Hirsch, *Angew. Chem., Int. Ed.*, 2014, **53**, 7720–7738.
43 R. K. Joshi, S. Alwarappan, M. Yoshimura, V. Sahajwalla and Y. Nishina, *Appl. Mater. Today*, 2015, **1**, 1–12.
44 R. Narayan, J. E. Kim, J. Y. Kim, K. E. Lee and S. O. Kim, *Adv. Mater.*, 2016, **28**, 3045–3068.
45 N. Morimoto, H. Suzuki, Y. Takeuchi, S. Kawaguchi, M. Kunisu, C. W. Bielawski and Y. Nishina, *Chem. Mater.*, 2017, **29**, 2150–2156.
46 S. P. Sasikala, J. Lim, I. H. Kim, H. J. Jung, T. Yun, T. H. Han and S. O. Kim, *Chem. Soc. Rev.*, 2018, **47**, 6013–6045.
47 M. Z. I. Nizami, S. Takashiba and Y. Nishina, *Appl. Mater. Today*, 2020, **19**, 100576.
48 F. Lin, Z. Zhu, X. Zhou, W. Qiu, C. Niu, J. Hu, K. Dahal, Y. Wang, Z. Zhao, Z. Ren, D. Litvinov, Z. Liu, Z. M. Wang and J. Bao, *Adv. Mater.*, 2017, **29**, 1604453.
49 B. Tian, W. Lin, P. Zhuang, J. Li, T.-m. Shih and W. Cai, *Carbon*, 2018, **131**, 66–71.
50 F. Lin, G. Yang, C. Niu, Y. Wang, Z. Zhu, H. Luo, C. Dai, D. Mayerich, Y. Hu, J. Hu, X. Zhou, Z. Liu, Z. M. Wang and J. Bao, *Adv. Funct. Mater.*, 2018, **28**, 1805255.
51 L. Wu, M. Ohtani, M. Takata, A. Saeki, S. Seki, Y. Ishida and T. Aida, *ACS Nano*, 2014, **8**, 4640–4649.
52 X. Lu, X. Feng, J. R. Werber, C. Chu, I. Zucker, J.-H. Kim, C. O. Osuji and M. Elimelech, *Proc. Natl. Acad. Sci. U. S. A.*, 2017, **114**, E9793–E9801.
53 X. Wang, Z. Li, S. Wang, K. Sano, Z. Sun, Z. Shao, A. Takeishi, S. Matsubara, D. Okumura, N. Sakai, T. Aida and Y. Ishida, *Science*, 2023, **380**, 192–198.
54 L. Pauling, *J. Chem. Phys.*, 1936, **4**, 673–677.